Eur. Phys. J. C 40, 505–514 (2005)
Digital Object Identifier (DOI) 10.1140/epjc/s2005-02150-0

THE EUROPEAN PHYSICAL JOURNAL C

# Polarized forward–backward asymmetries of leptons in $B_s \to \ell^+\ell^-\gamma$ decay

T.M. Aliev[a], V. Bashiry[b], M. Savcı[c]

Physics Department, Middle East Technical University, 06531 Ankara, Turkey

Received: 27 December 2004 / Revised version: 25 January 2005 /
Published online: 9 March 2005 – 

**Abstract.** Polarized forward–backward asymmetries in the $B_s \to \ell^+\ell^-\gamma$ decay are calculated using the most general, model independent form of the effective Hamiltonian, including all possible forms of interactions. The dependencies of the asymmetries on new Wilson coefficients are investigated. The detectability of the asymmetries at LHC is discussed.

**PACS.** 12.60.-i, 13.30.-a

## 1 Introduction

Rare radiative leptonic $B_{s(d)} \to \ell^+\ell^-\gamma$ decays are induced by the flavor-changing neutral current transitions $b \to s(d)$. In the standard model (SM) such processes are described by penguin and box diagrams and have branching ratios $10^{-8}$–$10^{-15}$ (see for example [1]). These rare decays cannot be observed at the running machines such as Tevatron, BaBar and Belle, but the $B_{s(d)} \to \mu^+\mu^-$ and $B_{s(d)} \to \mu^+\mu^-\gamma$ decays can be detected at LHC with ATLAS, CMS and LHCb detectors [2]. Many experimental observables such as the branching ratio, photon energy, dilepton mass spectra and charge asymmetries, as well as the transition form factors, are investigated for the $B_{s(d)} \to \ell^+\ell^-\gamma$ decays in [3–9]. At the same time $B_{s(d)} \to \ell^+\ell^-\gamma$ decays might be sensitive to new physics beyond the SM. New physics effects in these decays can appear in two different ways: either through the new operators in the effective Hamiltonian which are absent in the SM, or through new contributions to the Wilson coefficients existing in the SM. One efficient way for the precise determination of the SM parameters and looking for new physics beyond the SM is studying the lepton polarization effects. It has been pointed out in [10] that some of the single lepton polarization asymmetries might be too small to be observed and might not provide a sufficient number of observables in checking the structure of the effective Hamiltonian. In need of more observables, in [10] a maximum number of independent observables have been constructed by considering the situation where both lepton polarizations are simultaneously measured.

In the present work, we analyze the possibility of searching for new physics in the $B_s \to \ell^+\ell^-\gamma$ decay by studying the forward–backward asymmetries when both leptons are polarized, using the most general, model independent form of the effective Hamiltonian including all possible interactions. Note that the sensitivity of double-lepton polarization asymmetries on new Wilson coefficients for the $B_s \to \ell^+\ell^-\gamma$ decay has been investigated recently in [11].

This work is organized as follows. In Sect. 2, the matrix element for the $B_s \to \ell^+\ell^-\gamma$ is obtained, using the general, model independent form of the effective Hamiltonian. In Sect. 3, we calculate the polarized forward–backward asymmetries of the leptons in $B_s \to \ell^+\ell^-\gamma$ decay. Section 4 is devoted to the numerical analysis, discussions and conclusions.

## 2 Theoretical framework

In the present section we derive the matrix element for the $B_s \to \ell^+\ell^-\gamma$ using the general, model independent form of the effective Hamiltonian. The matrix element for the process $B_s \to \ell^+\ell^-\gamma$ can be obtained from that of the purely leptonic $B_s \to \ell^+\ell^-$ decay. At inclusive level the process $B_s \to \ell^+\ell^-$ is described by the $b \to q\ell^+\ell^-$ transition. The effective $b \to q\ell^+\ell^-$ transition can be written in terms of twelve model independent four-Fermi interactions in the following form [12]:

$$\begin{aligned}\mathcal{H}_{\rm eff} &= \frac{G\alpha}{\sqrt{2}\pi} V_{tq} V_{tb}^* \\ &\times \Big\{ C_{\rm SL}\, \bar{q} \mathrm{i}\sigma_{\mu\nu} \frac{q^\nu}{q^2} L\, b\, \bar{\ell}\gamma^\mu \ell + C_{\rm BR}\, \bar{q} \mathrm{i}\sigma_{\mu\nu} \frac{q^\nu}{q^2} R\, b\, \bar{\ell}\gamma^\mu \ell \\ &+ C_{\rm LL}^{\rm tot}\, \bar{q}\gamma_\mu L b\, \bar{\ell}\gamma^\mu L \ell + C_{\rm LR}^{\rm tot}\, \bar{q}\gamma_\mu L b\, \bar{\ell}\gamma^\mu R \ell \\ &+ C_{\rm RL}\, \bar{q}\gamma_\mu R b\, \bar{\ell}\gamma^\mu L \ell + C_{\rm RR}\, \bar{q}\gamma_\mu R b\, \bar{\ell}\gamma^\mu R \ell \\ &+ C_{\rm LRLR}\, \bar{q} R b\, \bar{\ell} R \ell + C_{\rm RLLR}\, \bar{q} L b\, \bar{\ell} R \ell\end{aligned}$$

[a] e-mail: taliev@metu.edu
[b] e-mail: bashiry@newton.physics.metu.edu.tr
[c] e-mail: savci@metu.edu

$$+C_{\rm LRRL}\,\bar{q}Rb\,\bar{\ell}L\ell + C_{\rm RLRL}\,\bar{q}Lb\,\bar{\ell}L\ell$$
$$+C_{\rm T}\,\bar{q}\sigma_{\mu\nu}b\,\bar{\ell}\sigma^{\mu\nu}\ell + {\rm i}C_{\rm TE}\,\epsilon^{\mu\nu\alpha\beta}\bar{q}\sigma_{\mu\nu}b\,\bar{\ell}\sigma_{\alpha\beta}\ell\Big\}, \qquad (1)$$

where $C_X$ are the coefficients of the four-Fermi interactions and

$$L = \frac{1-\gamma_5}{2}, \quad R = \frac{1+\gamma_5}{2}.$$

The terms with coefficients $C_{\rm SL}$ and $C_{\rm BR}$ which describe penguin contributions correspond to $-2m_sC_7^{\rm eff}$ and $-2m_bC_7^{\rm eff}$ in the SM, respectively. The next four terms in this expression are the vector interactions. The interaction terms containing $C_{\rm LL}^{\rm tot}$ and $C_{\rm LR}^{\rm tot}$ in the SM have the form $C_9^{\rm eff} - C_{10}$ and $C_9^{\rm eff} + C_{10}$, respectively. Inspired by this, $C_{\rm LL}^{\rm tot}$ and $C_{\rm LR}^{\rm tot}$ will be written as

$$C_{\rm LL}^{\rm tot} = C_9^{\rm eff} - C_{10} + C_{\rm LL},$$
$$C_{\rm LR}^{\rm tot} = C_9^{\rm eff} + C_{10} + C_{\rm LR},$$

where $C_{\rm LL}$ and $C_{\rm LR}$ describe contributions from new physics. The terms with coefficients $C_{\rm LRLR}, C_{\rm RLLR}, C_{\rm LRRL}$ and $C_{\rm RLRL}$ describe the scalar type interactions. The last two terms in (1) with the coefficients $C_{\rm T}$ and $C_{\rm TE}$ describe the tensor type interactions.

Having presented the general form of the effective Hamiltonian the next problem is the calculation of the matrix element of the $B_q \to \ell^+\ell^-\gamma$ decay. This matrix element can be written as the sum of the two parts, structure-dependent and inner-Bremsstrahlung parts

$$\mathcal{M} = \mathcal{M}_{\rm SD} + \mathcal{M}_{\rm IB}. \qquad (2)$$

The matrix element for the structure-dependent part $\mathcal{M}_{\rm SD}$, which corresponds to the radiation of photon from initial quarks, can be obtained by calculating the matrix element $\langle\gamma\,|\mathcal{H}_{\rm eff}|\,B\rangle$. Using (1) we see that for calculation of $\mathcal{M}_{\rm SD}$ we need to know the following matrix elements:

$$\langle\gamma\,|\bar{s}\gamma_\mu(1\mp\gamma_5)b|\,B\rangle,$$
$$\langle\gamma\,|\bar{s}\sigma_{\mu\nu}q^\nu b|\,B\rangle,$$
$$\langle\gamma\,|\bar{s}\sigma_{\mu\nu}b|\,B\rangle,$$
$$\langle\gamma\,|\bar{s}(1\mp\gamma_5)b|\,B\rangle. \qquad (3)$$

The first two of the matrix elements in (3) are defined in the following way [3,7,13,14]:

$$\langle\gamma(k)\,|\bar{q}\gamma_\mu(1\mp\gamma_5)b|\,B(p_B)\rangle$$
$$= \frac{e}{m_B^2}\left\{\epsilon_{\mu\nu\lambda\sigma}\varepsilon^{*\nu}q^\lambda k^\sigma g(q^2)\right.$$
$$\left. \pm{\rm i}\left[\varepsilon^{*\mu}(kq) - (\varepsilon^* q)k^\mu\right]f(q^2)\right\}, \qquad (4)$$

$$\langle\gamma(k)\,|\bar{q}\sigma_{\mu\nu}b|\,B(p_B)\rangle$$
$$= \frac{e}{m_B^2}\epsilon_{\mu\nu\lambda\sigma}\left[G\varepsilon^{*\lambda}k^\sigma + H\varepsilon^{*\lambda}q^\sigma + N(\varepsilon^* q)q^\lambda k^\sigma\right]. \qquad (5)$$

Here, $\varepsilon^*$ and $k$ are the four vector polarization and momentum of the photon, respectively, $q = p_B - k$ is the momentum transfer, $p_B$ is the momentum of the $B$ meson and $g(q^2), f(q^2), G(q^2), H(q^2)$ and $N(q^2)$ are the $B_s \to \gamma$ transition form factors. The matrix element $\langle\gamma(k)|\bar{s}\sigma_{\mu\nu}\gamma_5 b|B(p_B)\rangle$ can be obtained from (5) using the identity

$$\sigma_{\mu\nu} = -\frac{\rm i}{2}\epsilon_{\mu\nu\alpha\beta}\sigma^{\alpha\beta}\gamma_5.$$

The matrix elements

$$\langle\gamma(k)\,|\bar{s}(1\mp\gamma_5)b|\,B(p_B)\rangle$$
and
$$\langle\gamma\,|\bar{s}{\rm i}\sigma_{\mu\nu}q^\nu b|\,B\rangle$$

can be obtained from (4) and (5) by multiplying them by $q^\mu$ and $q^\nu$, respectively, as a result of which we get

$$\langle\gamma(k)\,|\bar{s}(1\mp\gamma_5)b|\,B(p_B)\rangle = 0, \qquad (6)$$

$$\langle\gamma\,|\bar{s}{\rm i}\sigma_{\mu\nu}q^\nu b|\,B\rangle = \frac{e}{m_B^2}{\rm i}\,\epsilon_{\mu\nu\alpha\beta}q^\nu\varepsilon^{\alpha*}k^\beta G. \qquad (7)$$

The matrix element $\langle\gamma\,|\bar{s}{\rm i}\sigma_{\mu\nu}q^\nu(1+\gamma_5)b|\,B\rangle$ can be written in terms of the two form factors $f_1(q^2)$ and $g_1(q^2)$ that are calculated in the framework of QCD sum rules [3,13] in the following way:

$$\langle\gamma\,|\bar{s}{\rm i}\sigma_{\mu\nu}q^\nu(1+\gamma_5)b|\,B\rangle$$
$$= \frac{e}{m_B^2}\left\{\epsilon_{\mu\alpha\beta\sigma}\,\varepsilon^{\alpha*}q^\beta k^\sigma g_1(q^2)\right.$$
$$\left. +{\rm i}\,\left[\varepsilon_\mu^*(qk) - (\varepsilon^* q)k_\mu\right]f_1(q^2)\right\}. \qquad (8)$$

It should be noted that these form factors were calculated in the framework of the light-front model in [14]. Equations (5), (7) and (8) allow us to express $G$, $H$ and $N$ in terms of $f_1$ and $g_1$. Equations (4)–(8) help us rewrite $\mathcal{M}_{\rm SD}$ in the following form:

$$\mathcal{M}_{\rm SD} = \frac{\alpha G_{\rm F}}{4\sqrt{2}\,\pi}V_{tb}V_{tq}^*$$
$$\times\frac{e}{m_B^2}\left\{\bar{\ell}\gamma^\mu(1-\gamma_5)\ell\right.$$
$$\times\left[A_1\epsilon_{\mu\nu\alpha\beta}\varepsilon^{*\nu}q^\alpha k^\beta + {\rm i}\,A_2\left(\varepsilon_\mu^*(kq) - (\varepsilon^* q)k_\mu\right)\right]$$
$$+\bar{\ell}\gamma^\mu(1+\gamma_5)\ell$$
$$\times\left[B_1\epsilon_{\mu\nu\alpha\beta}\varepsilon^{*\nu}q^\alpha k^\beta + {\rm i}\,B_2\left(\varepsilon_\mu^*(kq) - (\varepsilon^* q)k_\mu\right)\right]$$
$$+{\rm i}\,\epsilon_{\mu\nu\alpha\beta}\bar{\ell}\sigma^{\mu\nu}\ell\,\left[G\varepsilon^{*\alpha}k^\beta + H\varepsilon^{*\alpha}q^\beta + N(\varepsilon^* q)q^\alpha k^\beta\right]$$
$$+{\rm i}\,\bar{\ell}\sigma_{\mu\nu}\ell$$
$$\left.\times\left[G_1(\varepsilon^{*\mu}k^\nu - \varepsilon^{*\nu}k^\mu) + H_1(\varepsilon^{*\mu}q^\nu - \varepsilon^{*\nu}q^\mu)\right.\right.$$
$$\left.\left.+N_1(\varepsilon^* q)(q^\mu k^\nu - q^\nu k^\mu)\right]\right\}, \qquad (9)$$

where

$$A_1 = \frac{1}{q^2}\left(C_{\rm BR} + C_{\rm SL}\right)g_1 + \left(C_{\rm LL}^{\rm tot} + C_{\rm RL}\right)g,$$

$$A_2 = \frac{1}{q^2}\left(C_{\rm BR} - C_{\rm SL}\right)f_1 + \left(C_{\rm LL}^{\rm tot} - C_{\rm RL}\right)f,$$

$$B_1 = \frac{1}{q^2}\left(C_{\rm BR} + C_{\rm SL}\right)g_1 + \left(C_{\rm LR}^{\rm tot} + C_{\rm RR}\right)g,$$

$$
\begin{aligned}
B_2 &= \frac{1}{q^2}\left(C_{\rm BR} - C_{\rm SL}\right) f_1 + \left(C_{\rm LR}^{\rm tot} - C_{\rm RR}\right) f,\\
G &= 4C_{\rm T} g_1,\\
N &= -4C_{\rm T}\frac{1}{q^2}(f_1+g_1),\\
H &= N(qk),\\
G_1 &= -8C_{\rm TE} g_1,\\
N_1 &= 8C_{\rm TE}\frac{1}{q^2}(f_1+g_1),\\
H_1 &= N_1(qk).
\end{aligned}
\tag{10}
$$

In regard to the inner-Bremsstrahlung part, as a result of the relevant calculations we get

$$
\begin{aligned}
\mathcal{M}_{\rm IB} = \frac{\alpha G_{\rm F}}{4\sqrt{2}\,\pi} V_{tb}V_{tq}^* e f_B {\rm i}\left\{F\,\bar{\ell}\left(\frac{\not{\varepsilon}^*\not{p}_B}{2p_1k} - \frac{\not{p}_B\not{\varepsilon}^*}{2p_2k}\right)\gamma_5\ell\right.\\
\left. + F_1\,\bar{\ell}\left[\frac{\not{\varepsilon}^*\not{p}_B}{2p_1k} - \frac{\not{p}_B\not{\varepsilon}^*}{2p_2k} + 2m_\ell\left(\frac{1}{2p_1k}+\frac{1}{2p_2k}\right)\not{\varepsilon}^*\right]\ell\right\}.
\end{aligned}
\tag{11}
$$

In deriving (11), we have used

$$
\begin{aligned}
\langle 0|\bar{s}\gamma_\mu\gamma_5 b|B\rangle &= -{\rm i} f_B p_{B\mu},\\
\langle 0|\bar{s}\sigma_{\mu\nu}(1+\gamma_5)b|B\rangle &= 0,
\end{aligned}
$$

The functions $F$ and $F_1$ are defined as follows

$$
\begin{aligned}
F &= 2m_\ell\left(C_{\rm LR}^{\rm tot} - C_{\rm LL}^{\rm tot} + C_{\rm RL} - C_{\rm RR}\right)\\
&\quad + \frac{m_B^2}{m_b}\left(C_{\rm LRLR} - C_{\rm RLLR} - C_{\rm LRRL} + C_{\rm RLRL}\right),\\
F_1 &= \frac{m_B^2}{m_b}\left(C_{\rm LRLR} - C_{\rm RLLR} + C_{\rm LRRL} - C_{\rm RLRL}\right).
\end{aligned}
\tag{12}
$$

## 3 Polarized forward–backward asymmetries of the leptons in $B_s \to \ell^+\ell^-\gamma$ decay

In the present section we calculate the polarized forward–backward asymmetries of leptons. For this purpose we define the following orthogonal unit vectors $s_i^\pm$ (here $i$ = L, T or N stands for longitudinal, transversal or normal polarizations, respectively) in the rest frame of $\ell^\pm$

$$
\begin{aligned}
s_{\rm L}^{-\mu} &= \left(0, \boldsymbol{e}_{\rm L}^-\right) = \left(0, \frac{\boldsymbol{p}_-}{|\boldsymbol{p}_-|}\right),\\
s_{\rm N}^{-\mu} &= \left(0, \boldsymbol{e}_{\rm N}^-\right) = \left(0, \frac{\boldsymbol{p}_\Lambda\times\boldsymbol{p}_-}{|\boldsymbol{p}_\Lambda\times\boldsymbol{p}_-|}\right),\\
s_{\rm T}^{-\mu} &= \left(0, \boldsymbol{e}_{\rm T}^-\right) = \left(0, \boldsymbol{e}_{\rm N}^-\times\boldsymbol{e}_{\rm L}^-\right),\\
s_{\rm L}^{+\mu} &= \left(0, \boldsymbol{e}_{\rm L}^+\right) = \left(0, \frac{\boldsymbol{p}_+}{|\boldsymbol{p}_+|}\right),\\
s_{\rm N}^{+\mu} &= \left(0, \boldsymbol{e}_{\rm N}^+\right) = \left(0, \frac{\boldsymbol{p}_\Lambda\times\boldsymbol{p}_+}{|\boldsymbol{p}_\Lambda\times\boldsymbol{p}_+|}\right),
\end{aligned}
$$

$$
s_{\rm T}^{+\mu} = \left(0, \boldsymbol{e}_{\rm T}^+\right) = \left(0, \boldsymbol{e}_{\rm N}^+\times\boldsymbol{e}_{\rm L}^+\right),
\tag{13}
$$

where $\boldsymbol{p}_\pm$ and $\boldsymbol{k}$ are the three-momenta of the leptons $\ell^\pm$ and photon in the center of mass frame (CM) of $\ell^-\,\ell^+$ system, respectively. Transformation of unit vectors from the rest frame of the leptons to CM frame of leptons can be accomplished by the Lorentz boost. Boosting of the longitudinal unit vectors $s_{\rm L}^{\pm\mu}$ yields

$$
\left(s_{\rm L}^{\mp\mu}\right)_{\rm CM} = \left(\frac{|\boldsymbol{p}_\mp|}{m_\ell}, \frac{E_\ell \boldsymbol{p}_\mp}{m_\ell\,|\boldsymbol{p}_\mp|}\right),
\tag{14}
$$

where $\boldsymbol{p}_+ = -\boldsymbol{p}_-$, $E_\ell$ and $m_\ell$ are the energy mass of leptons in the CM frame. The remaining unit vectors $s_{\rm N}^{\pm\mu}$, $s_{\rm T}^{\pm\mu}$ are unchanged under a Lorentz transformation.

The definition of the normalized, unpolarized differential forward–backward asymmetry is

$$
\mathcal{A}_{\rm FB} = \frac{\displaystyle\int_0^1 {\rm d}z\frac{{\rm d}^2\Gamma}{{\rm d}\hat{s}{\rm d}z} - \int_{-1}^0 {\rm d}z\frac{{\rm d}^2\Gamma}{{\rm d}\hat{s}{\rm d}z}}{\displaystyle\int_0^1 {\rm d}z\frac{{\rm d}^2\Gamma}{{\rm d}\hat{s}{\rm d}z} + \int_{-1}^0 {\rm d}z\frac{{\rm d}^2\Gamma}{{\rm d}\hat{s}{\rm d}z}},
\tag{15}
$$

where $z = \cos\theta$ is the angle between $\Lambda_b$ meson and $\ell^-$ in the center of mass frame of the leptons. When the spins of both leptons are taken into account, the $\mathcal{A}_{\rm FB}$ will be a function of the spins of the final leptons, and it is defined as

$$
\begin{aligned}
&\mathcal{A}_{\rm FB}^{ij}(\hat{s})\\
&= \left(\frac{{\rm d}\Gamma(\hat{s})}{{\rm d}\hat{s}}\right)^{-1}\left\{\int_0^1 {\rm d}z - \int_{-1}^0 {\rm d}z\right\}\\
&\quad\times\left\{\left[\frac{{\rm d}^2\Gamma(\hat{s}, \boldsymbol{s}^- = \boldsymbol{i}, \boldsymbol{s}^+ = \boldsymbol{j})}{{\rm d}\hat{s}{\rm d}z}\right.\right.\\
&\quad\left.- \frac{{\rm d}^2\Gamma(\hat{s}, \boldsymbol{s}^- = \boldsymbol{i}, \boldsymbol{s}^+ = -\boldsymbol{j})}{{\rm d}\hat{s}{\rm d}z}\right]\\
&\quad- \left[\frac{{\rm d}^2\Gamma(\hat{s}, \boldsymbol{s}^- = -\boldsymbol{i}, \boldsymbol{s}^+ = \boldsymbol{j})}{{\rm d}\hat{s}{\rm d}z}\right.\\
&\quad\left.\left.- \frac{{\rm d}^2\Gamma(\hat{s}, \boldsymbol{s}^- = -\boldsymbol{i}, \boldsymbol{s}^+ = -\boldsymbol{j})}{{\rm d}\hat{s}{\rm d}z}\right]\right\},\\
&= \mathcal{A}_{\rm FB}(\boldsymbol{s}^- = \boldsymbol{i}, \boldsymbol{s}^+ = \boldsymbol{j}) - \mathcal{A}_{\rm FB}(\boldsymbol{s}^- = \boldsymbol{i}, \boldsymbol{s}^+ = -\boldsymbol{j})\\
&\quad - \mathcal{A}_{\rm FB}(\boldsymbol{s}^- = -\boldsymbol{i}, \boldsymbol{s}^+ = \boldsymbol{j})\\
&\quad + \mathcal{A}_{\rm FB}(\boldsymbol{s}^- = -\boldsymbol{i}, \boldsymbol{s}^+ = -\boldsymbol{j}).
\end{aligned}
\tag{16}
$$

Using these definitions for the double polarized FB asymmetries, we get the following results:

$$
\begin{aligned}
\mathcal{A}_{\rm FB}^{\rm LL} &= \frac{1}{\Delta}\left\{-4m_B^2\hat{s}(1-\hat{s})^2 v\,{\rm Re}[A_1^*A_2 - B_1^*B_2]\right.\\
&\quad - \frac{2}{\hat{m}_\ell} m_B\hat{s}(1-\hat{s})^2 v(1-v^2)\\
&\quad\times\left({\rm Im}[(A_1^* - B_1^*)G_1] - {\rm Re}[(A_2 - B_2)^* G]\right)\\
&\quad\left. - \frac{4}{\hat{m}_\ell} m_B\hat{s}^2(1-\hat{s}) v(1-v^2)\,{\rm Im}[(A_1^* - B_1^*)H_1]\right.
\end{aligned}
$$

$$
\begin{aligned}
&+\frac{4}{\hat{m}_\ell v} f_B m_B \hat{s}(1-\hat{s})(1-v^2)\ln[1-v^2]\\
&\times \mathrm{Re}[(A_2^*-B_2^*)F]\\
&-\frac{4}{\hat{m}_\ell v} f_B m_B \hat{s}(1-\hat{s})(1-v^2)\ln[1-v^2]\\
&\times \mathrm{Re}[(A_1^*-B_1^*)F_1]\Big\}, \qquad (17)
\end{aligned}
$$

$$
\begin{aligned}
\mathcal{A}_{\rm FB}^{\rm LN} = \frac{1}{\Delta}\Big\{&-\frac{4}{3} m_B\sqrt{\hat{s}}(1-\hat{s})^2 v\\
&\times \mathrm{Re}[(A_1^*-A_2^*+B_1^*+B_2^*)G_1]\\
&+\frac{4}{3} m_B\sqrt{\hat{s}}(1-\hat{s})^2 v\,\mathrm{Im}[(A_1^*-A_2^*-B_1^*-B_2^*)G]\\
&+\frac{4}{3} m_B^3\sqrt{\hat{s}^3}(1-\hat{s})^2 v\\
&\times (\mathrm{Re}[(A_2^*-B_2^*)N_1^*]-\mathrm{Im}[(A_2^*+B_2^*)N])\\
&-\frac{2}{3\hat{m}_\ell} m_B^2\sqrt{\hat{s}^3}(1-\hat{s})^2 v(1-v^2)\\
&\times \big(2\,\mathrm{Re}[G^* N_1+G_1^* N+m_B^2\hat{s}N_1^* N]\\
&+\mathrm{Im}[A_1^* B_1+A_2^* B_2]\big)\\
&-f_B m_B^2\sqrt{\hat{s}}(1-\hat{s})\\
&\times\big\{2 f_B m_B^2\hat{m}_\ell\,\mathrm{Im}[F_1^* F]I_4\\
&+v\,[m_B(1-\hat{s})\,\mathrm{Im}[(A_1^*+B_1^*)F_1]\\
&+m_B\,\mathrm{Im}[(A_1^*-A_2^*-B_1^*-B_2^*)F\\
&-\hat{s}(A_1^*+A_2^*-B_1^*+B_2^*)F]+8\hat{m}_\ell\,\mathrm{Re}[F^* H_1]]\,I_7\ \}\\
&+f_B m_B^3\sqrt{\hat{s}}(1-\hat{s})\\
&\times v[1-\hat{s}(1-2v^2)]\,\mathrm{Im}[(A_2^*-B_2^*)F_1]\mathcal{J}_4\\
&+8 f_B m_B^2\hat{m}_\ell\sqrt{\hat{s}}(1-\hat{s})v\,\mathrm{Re}[F^*(G_1+m_B^2 N_1)]\mathcal{J}_4\\
&+4 f_B m_B^4\hat{m}_\ell\sqrt{\hat{s}}(1-\hat{s})^2 v\,\mathrm{Im}[F_1^* N]\mathcal{J}_4\Big\}, \qquad (18)
\end{aligned}
$$

$$
\begin{aligned}
\mathcal{A}_{\rm FB}^{\rm NL} = \frac{1}{\Delta}\Big\{&\frac{4}{3} m_B\sqrt{\hat{s}}(1-\hat{s})^2 v\\
&\times \mathrm{Re}[(A_1^*+A_2^*+B_1^*-B_2^*)G_1]\\
&+\frac{4}{3} m_B\sqrt{\hat{s}}(1-\hat{s})^2 v\,\mathrm{Im}[(A_1^*+A_2^*-B_1^*+B_2^*)G]\\
&+\frac{4}{3} m_B^3\sqrt{\hat{s}^3}(1-\hat{s})^2\\
&\times v\,(\mathrm{Re}[(A_2^*-B_2^*)N_1]+\mathrm{Im}[(A_2^*+B_2^*)N])\\
&+\frac{2}{3\hat{m}_\ell} m_B^2\sqrt{\hat{s}^3}(1-\hat{s})^2 v(1-v^2)\\
&\times \big(2\,\mathrm{Re}[G^* N_1+G_1^* N+m_B^2\hat{s}N_1^* N]\\
&-\mathrm{Im}[A_1^* B_1+A_2^* B_2]\big)\\
&+f_B m_B^2\sqrt{\hat{s}}(1-\hat{s})\\
&\times\big\{2 f_B m_B^2\hat{m}_\ell\,\mathrm{Im}[F_1^* F]I_4\\
&+v\,[m_B(1-\hat{s})\,\mathrm{Im}[(A_1^*+B_1^*)F_1]\\
&-m_B\,\mathrm{Im}[(A_1^*+A_2^*-B_1^*+B_2^*)F\\
&-\hat{s}(A_1^*-A_2^*-B_1^*-B_2^*)F]+8\hat{m}_\ell\,\mathrm{Re}[F^* H_1]]\,I_7\ \}\\
&+f_B m_B^3\sqrt{\hat{s}}(1-\hat{s})v[1-\hat{s}(1-2v^2)]\\
&\times \mathrm{Im}[(A_2^*-B_2^*)F_1]\mathcal{J}_4\\
&-8 f_B m_B^2\hat{m}_\ell\sqrt{\hat{s}}(1-\hat{s})v\,\mathrm{Re}[F^*(G_1+m_B^2 N_1)]\mathcal{J}_4\\
&-4 f_B m_B^4\hat{m}_\ell\sqrt{\hat{s}}(1-\hat{s})^2 v\,\mathrm{Im}[F_1^* N]\mathcal{J}_4\Big\}, \qquad (19)
\end{aligned}
$$

$$
\begin{aligned}
\mathcal{A}_{\rm FB}^{\rm LT} = \frac{1}{\Delta}\Big\{&\frac{4}{3\sqrt{\hat{s}}}\hat{m}_\ell(1-\hat{s})^2\Big[4\left(|G_1|^2+|G|^2\right)\\
&+m_B^2\hat{s}\left(|A_1|^2+|A_2|^2+|B_1|^2+|B_2|^2\right)\Big]\\
&-\frac{4}{3} m_B\sqrt{\hat{s}}(1-\hat{s})^2 v^2\,(\mathrm{Im}[(A_1^*-B_1^*)G_1]\\
&-\mathrm{Re}[(A_2^*-B_2^*)(G+m_B^2\hat{s}N)])\\
&-\frac{4}{3} m_B\sqrt{\hat{s}}(1-\hat{s})^2(2-v^2)\,(?\,\mathrm{Re}[(A_1^*+B_1^*)G]\\
&-\mathrm{Im}[(A_2^*+B_2^*)\left(G_1+m_B^2\hat{s}N_1\right)])\\
&+\frac{8}{3} m_B^2\hat{m}_\ell\sqrt{\hat{s}}(1-\hat{s})^2\\
&\times\left(\mathrm{Re}[A_1^* B_1+A_2^* B_2+4G_1^* N_1]+2m_B^2\hat{s}\,|N_1|^2\right)\\
&+\frac{1}{\sqrt{\hat{s}}} f_B^2 m_B^4\hat{m}_\ell(1-\hat{s})\\
&\times\left[(1-\hat{s})\left(|F_1|^2+|F|^2\right)(\mathcal{J}_1+\mathcal{J}_2)+2\hat{s}v\,|F_1|^2\,\mathcal{J}_3\right]\\
&+f_B m_B^3\sqrt{\hat{s}}(1-\hat{s})^2 v^2\,\mathrm{Re}[(A_1^*-B_1^*)F_1]\mathcal{J}_4\\
&-f_B m_B^3\sqrt{\hat{s}}(1-\hat{s}^2)v^2\,\mathrm{Re}[(A_2^*-B_2^*)F^*]\mathcal{J}_4\\
&+f_B m_B^3\sqrt{\hat{s}}(1-\hat{s})^2(2-v^2)\,\mathrm{Re}[(A_1^*+B_1^*)F]\mathcal{J}_4\\
&-4 f_B m_B^4\hat{m}_\ell\sqrt{\hat{s}}(1-\hat{s})[2+v^2-\hat{s}(2-v^2)]\\
&\times \mathrm{Im}[F_1^* N_1]\mathcal{J}_4\\
&+8 f_B m_B^2\hat{m}_\ell\sqrt{\hat{s}}(1-\hat{s})v^2\,\mathrm{Im}[F_1^* H_1]\mathcal{J}_4\\
&-f_B m_B^3\sqrt{\hat{s}}(1-\hat{s})[2-v^2-\hat{s}(2-3v^2)]\\
&\times \mathrm{Re}[(A_2^*+B_2^*)F_1]\mathcal{J}_4\\
&-\frac{8}{\sqrt{\hat{s}}} f_B m_B^2\hat{m}_\ell(1-\hat{s})\left[(1-\hat{s}+\hat{s}v^2)\,\mathrm{Im}[F_1^* G_1]\right.\\
&\left.+(1-\hat{s})\,\mathrm{Re}[F^* G]\right]\mathcal{J}_4\Big\}, \qquad (20)
\end{aligned}
$$

$$
\begin{aligned}
\mathcal{A}_{\rm FB}^{\rm TL} = \frac{1}{\Delta}\Big\{&-\frac{4}{3\sqrt{\hat{s}}}\hat{m}_\ell(1-\hat{s})^2\Big[4\left(|G_1|^2+|G|^2\right)\\
&+m_B^2\hat{s}\left(|A_1|^2+|A_2|^2+|B_1|^2+|B_2|^2\right)\Big]\\
&-\frac{4}{3} m_B\sqrt{\hat{s}}(1-\hat{s})^2 v^2
\end{aligned}
$$

$$
\begin{aligned}
&\times (\mathrm{Im}[(A_1^* - B_1^*)G_1] \\
&- \mathrm{Re}[(A_2^* - B_2^*)(G + m_B^2 \hat{s} N)]) \\
&+ \frac{4}{3} m_B \sqrt{\hat{s}} (1-\hat{s})^2 (2 - v^2) \\
&\times (\mathrm{Re}[(A_1^* + B_1^*)G] \\
&- \mathrm{Im}\left[(A_2^* + B_2^*)\left(G_1 + m_B^2 \hat{s} N_1\right)\right]) \\
&- \frac{8}{3} m_B^2 \hat{m}_\ell \sqrt{\hat{s}} (1-\hat{s})^2 \\
&\times \left(\mathrm{Re}[A_1^* B_1 + A_2^* B_2 + 4 G_1^* N_1] + 2 m_B^2 \hat{s} \left|N_1\right|^2\right) \\
&- \frac{1}{\sqrt{\hat{s}}} f_B^2 m_B^4 \hat{m}_\ell (1-\hat{s}) \\
&\times \left[(1-\hat{s})\left(\left|F_1\right|^2 + \left|F\right|^2\right)(\mathcal{J}_1 + \mathcal{J}_2) + 2\hat{s} v \left|F_1\right|^2 \mathcal{J}_3\right] \\
&+ f_B m_B^3 \sqrt{\hat{s}} (1-\hat{s})^2 v^2 \,\mathrm{Re}[(A_1^* - B_1^*)F_1]\mathcal{J}_4 \\
&- f_B m_B^3 \sqrt{\hat{s}} (1-\hat{s}^2) v^2 \,\mathrm{Re}[(A_2^* - B_2^*)F]\mathcal{J}_4 \\
&- f_B m_B^3 \sqrt{\hat{s}} (1-\hat{s})^2 (2 - v^2)\,\mathrm{Re}[(A_1^* + B_1^*)F]\mathcal{J}_4 \\
&+ 4 f_B m_B^4 \hat{m}_\ell \sqrt{\hat{s}} (1-\hat{s})[2 + v^2 - \hat{s}(2 - v^2)] \\
&\times \mathrm{Im}[F_1^* N_1]\mathcal{J}_4 \\
&- 8 f_B m_B^2 \hat{m}_\ell \sqrt{\hat{s}} (1-\hat{s}) v^2 \,\mathrm{Im}[F_1^* H_1]\mathcal{J}_4 \\
&+ f_B m_B^3 \sqrt{\hat{s}} (1-\hat{s})[2 - v^2 - \hat{s}(2 - 3v^2)] \\
&\times \mathrm{Re}[(A_2^* + B_2^*)F_1]\mathcal{J}_4 \\
&+ \frac{8}{\sqrt{\hat{s}}} f_B m_B^2 \hat{m}_\ell (1-\hat{s}) \left[(1 - \hat{s} + \hat{s} v^2)\,\mathrm{Im}[F_1^* G_1]\right. \\
&\left. + (1-\hat{s})\,\mathrm{Re}[F^* G]\right]\mathcal{J}_4\Bigg\}, \qquad (21)
\end{aligned}
$$

where

$$
\begin{aligned}
\Delta &= 16 m_B \hat{m}_\ell (1-\hat{s})^2 \left(\mathrm{Im}[(A_2^* + B_2^*)G_1]\right. \\
&\left. - \mathrm{Re}[(A_1^* + B_1^*)G - m_B \hat{m}_\ell (A_1^* B_1 + A_2^* B_2)]\right) \\
&+ 48 m_B \hat{m}_\ell \hat{s} (1-\hat{s})\,\mathrm{Im}[(A_2^* + B_2^*)H_1] \\
&- 8 m_B^3 \hat{m}_\ell \hat{s} (1-\hat{s})^2\,\mathrm{Im}[(A_2^* + B_2^*)N_1] \\
&+ \frac{2}{3}(1-\hat{s})^2 \left[4(3 - v^2)\left(\left|G_1\right|^2 + \left|G\right|^2\right)\right. \\
&\left. + m_B^2 \hat{s}(3 + v^2)\left(\left|A_1\right|^2 + \left|A_2\right|^2 + \left|B_1\right|^2 + \left|B_2\right|^2\right)\right] \\
&+ 16 \hat{s} v^2 \left[(1-\hat{s})\,\mathrm{Re}[G^* H] + \hat{s}\left|H\right|^2\right] \\
&+ 16 \hat{s}(3 - 2v^2)\left[(1-\hat{s})\,\mathrm{Re}[G_1^* H_1] + \hat{s}\left|H_1\right|^2\right] \\
&- \frac{4}{3} m_B^2 \hat{s}(1-\hat{s})^2 (3 - 2v^2)\left(2\,\mathrm{Re}[G_1^* N_1] + m_B^2 \hat{s}\left|N_1\right|^2\right) \\
&- \frac{4}{3} m_B^2 \hat{s}(1-\hat{s})^2 v^2 \left(2\,\mathrm{Re}[G^* N] + m_B^2 \hat{s}\left|N\right|^2\right) \\
&- \frac{1}{2} f_B^2 m_B^4 \left|F\right|^2 \\
&\times \left\{(1-\hat{s})^2 v^2 (\mathcal{I}_1 + \mathcal{I}_3) - (1 + \hat{s}^2 + 2\hat{s} v^2)\mathcal{I}_2\right. \\
&\left. - [1 - \hat{s}(4 - \hat{s} - 2v^2)]\mathcal{I}_5\right\} \\
&+ \frac{1}{2} f_B^2 m_B^4 \left|F_1\right|^2 \\
&\times \left\{-(1-\hat{s})^2 v^2 (\mathcal{I}_1 + \mathcal{I}_3)\right. \\
&+ [1 - \hat{s}(2 - \hat{s} - 4v^2 + 2\hat{s} v^2 - 2\hat{s} v^4)]\mathcal{I}_2 \\
&- 2\hat{s}(1-\hat{s}) v (1 - v^2)\mathcal{I}_4 \\
&\left. + [1 - \hat{s}(2 - \hat{s} + 2\hat{s} v^2 - 2\hat{s} v^4)]\mathcal{I}_5\right\} \\
&- 4 f_B m_B^2 \hat{s} v\,\mathrm{Re}[F^* H][(1-\hat{s}) v \mathcal{I}_6 + (1 + \hat{s})\mathcal{I}_7] \\
&- 4 f_B m_B^2 \hat{s}\,\mathrm{Im}[F_1^* H_1] \\
&\times [(1-\hat{s}) v^2 \mathcal{I}_6 + (3 - 2v^2 - 3\hat{s} + 4\hat{s} v^2)\mathcal{I}_7] \\
&+ 2 f_B m_B \hat{m}_\ell\,\mathrm{Re}[(A_1^* + B_1^*)F] \\
&\times \left[8(1 + \hat{s}) + m_B^2 (1 - \hat{s}^2) v^2 \mathcal{I}_6\right. \\
&\left. + m_B^2 (1-\hat{s})(1 - 3\hat{s})\mathcal{I}_7\right] \\
&- f_B m_B \hat{m}_\ell (1-\hat{s})\,\mathrm{Re}[(A_2^* + B_2^*)F_1] \\
&\times \left[8 + m_B^2 (1 - 5\hat{s}) v^2 \mathcal{I}_6 + m_B^2 (3 - 3\hat{s} + 4\hat{s} v^2)\mathcal{I}_7\right] \\
&+ f_B\,\mathrm{Im}[F_1^* G_1] \\
&\times \left[-24(1 - \hat{s} + 2\hat{s} v^2)\right. \\
&+ m_B^2 (1-\hat{s})(1 + 3\hat{s} - 6\hat{s} v^2) v^2 \mathcal{I}_6 \\
&\left. - m_B^2 (1-\hat{s})(1 - \hat{s} - 2\hat{s} v^2)\mathcal{I}_7\right] \\
&+ f_B\,\mathrm{Re}[F^* G] \\
&\times \left[-24(1 + \hat{s}) + m_B^2 (1-\hat{s})(1 - 3\hat{s}) v^2 \mathcal{I}_6\right. \\
&\left. - m_B^2 (1-\hat{s})(1 - 7\hat{s} + 4\hat{s} v^2)\mathcal{I}_7\right] \\
&+ f_B m_B^2 \hat{s}\,\mathrm{Im}[F_1^* N_1]\left[-8(1 - \hat{s} + 2\hat{s} v^2)\right. \\
&+ m_B^2 (1-\hat{s})(3 + \hat{s} - 2\hat{s} v^2) v^2 \mathcal{I}_6 \\
&\left. + m_B^2 (1-\hat{s})(3 - 2v^2 - 3\hat{s} + 4\hat{s} v^2)\mathcal{I}_7\right] \\
&+ f_B m_B^2 \hat{s}\,\mathrm{Re}[F^* N] \\
&\times \left[-8(1 + \hat{s}) + m_B^2 (1-\hat{s})(3 - \hat{s}) v^2 \mathcal{I}_6\right. \\
&\left. + m_B^2 (1 - \hat{s}^2)\mathcal{I}_7\right]. \qquad (22)
\end{aligned}
$$

In (16)–(22), $\hat{s} = q^2/m_B^2$, $v = \sqrt{1 - 4\hat{m}_\ell^2/\hat{s}}$ is the lepton velocity with $\hat{m}_\ell = m_\ell/m_B$, and $\mathcal{I}_i$ represent the following integrals:

$$
\begin{aligned}
\mathcal{I}_i &= \int_{-1}^{+1} \mathcal{F}_i(z)\mathrm{d}z, \\
\mathcal{J}_i &= \int_{0}^{+1} \mathcal{G}_i(z)\mathrm{d}z - \int_{-1}^{0} \mathcal{G}_i(z)\mathrm{d}z,
\end{aligned}
$$

where

$$
\mathcal{G}_1 = \frac{z\sqrt{1-z^2}}{(p_1 \cdot k)(p_2 \cdot k)}, \quad \mathcal{G}_2 = \frac{z\sqrt{1-z^2}}{(p_1 \cdot k)^2},
$$

$$\mathcal{G}_3 = \frac{\sqrt{1-z^2}}{(p_1\cdot k)^2}, \qquad \mathcal{G}_4 = \frac{z\sqrt{1-z^2}}{(p_1\cdot k)},$$
$$\mathcal{F}_1 = \frac{z^2}{(p_1\cdot k)(p_2\cdot k)}, \quad \mathcal{F}_2 = \frac{1}{(p_1\cdot k)(p_2\cdot k)},$$
$$\mathcal{F}_3 = \frac{z^2}{(p_1\cdot k)^2}, \qquad \mathcal{F}_4 = \frac{z}{(p_1\cdot k)^2},$$
$$\mathcal{F}_5 = \frac{1}{(p_1\cdot k)^2}, \qquad \mathcal{F}_6 = \frac{z^2}{p_1\cdot k},$$
$$\mathcal{F}_7 = \frac{1}{p_1\cdot k}.$$

We note that the forward–backward asymmetries $\mathcal{A}_{\rm NN}$, $\mathcal{A}_{\rm NT}$, $\mathcal{A}_{\rm TN}$ and $\mathcal{A}_{\rm TT}$ are all equal to zero.

## 4 Numerical analysis and discussion

In this section we present our numerical analysis for all possible polarized forward–backward asymmetries of leptons. The values of the input parameters which we have used in the numerical analysis are $|V_{tb}V_{ts}^*| = 0.0385$, $m_\mu = 0.106\,\text{GeV}$, $m_\tau = 1.78\,\text{GeV}$, $m_b = 4.8\,\text{GeV}$. For the SM values of the Wilson coefficients we have used $C_7^{\rm SM}(m_b) = -0.313$, $C_9^{\rm SM}(m_b) = 4.344$ which corresponds to the short distance contributions only, and $C_{10}^{\rm SM}(m_b) = -4.669$. The magnitude of $C_7^{\rm SM}$ is quite well determined from the $b \to s\gamma$ transition, and hence it is well established. Therefore the values of $C_{\rm BR}$ and $C_{\rm SL}$ are fixed by the relations $C_{\rm BR} = -2m_b C_7^{\rm eff}$ and $C_{\rm SL} = -2m_s C_7^{\rm eff}$. It is well known that the Wilson coefficient $C_9^{\rm SM}$ receives also long distance contributions which have their origin in the real $\bar{c}c$ intermediate states, i.e., $J/\psi$, $\psi'$, ... [15] that is realized as

$$C_9^{\rm eff} = C_9^{\rm SM} + Y(\hat{s}),$$

where

$$Y(\hat{s}) = Y^{\rm per}(\hat{s}) - \frac{3\pi}{\alpha^2}C^{(0)} \sum_{V_i=\psi(1s),\ldots,\psi(6s)} K_i \frac{\Gamma(V_i\to\ell^+\ell^-)m_{V_i}}{\hat{s}m_B^2 - m_{V_i}^2 + {\rm i}\Gamma_{V_i}m_{V_i}}.$$

Explicit expressions for $Y^{\rm per}(\hat{s})$, $C^{(0)}$ and the value of $K_i$ can be found in [16] and [17], respectively. In the present work we consider only short distance contributions.

A few comments about the long distance contributions are in order. It is well known that the dominant contributions arise from the first two low lying $J/\psi$ resonances. In order to minimize the hadronic uncertainties we must discard the kinematical region of $q^2$ between these two resonances by dividing it into low and high dilepton mass intervals as follows:

$$\begin{cases} \text{low } q^2 \text{ region}: & 4m_\ell^2 \le q^2 \le \left(m_\psi - \sqrt{\sqrt{2}\Gamma_\psi m_\psi}\right)^2, \\ \text{high } q^2 \text{ region}: & \left(m_{\psi'} + \sqrt{\sqrt{2}\Gamma_{\psi'} m_{\psi'}}\right)^2 \le q^2 \le m_{B_s}^2, \end{cases}$$

However, long distance contributions are negligibly small in the regions $R_1$ and $R_2$, and our analysis indeed confirms that the numerical results presented in this work almost coincide with the results when the long distance contributions are taken into account. This is a verification of the fact that our results are reliable and can safely be tested in the above-mentioned domains $R_1$ and $R_2$.

The values of the new Wilson coefficients are needed in order to carry out the numerical calculations for $\mathcal{A}_{ij}$ given in (17)–(22). All new Wilson coefficients are varied in the range $-\left|C_{10}^{\rm SM}\right| \le C_X \le \left|C_{10}^{\rm SM}\right|$ and it is assumed that they are real. The experimental results on the branching ratio of the $B \to K^*(K)\ell^+\ell^-$ decays [18,19] and the bound on the branching ratio of $B \to \mu^+\mu^-$ [20] suggest that this is the right order of magnitude for the Wilson coefficients describing the vector and scalar interaction coefficients. But present experimental results on the branching ratio of the $B \to K^*\ell^+\ell^-$ and $B \to K\ell^+\ell^-$ decays impose stronger restrictions on some of the new Wilson coefficients. For example, $-2 \le C_{\rm LL} \le 0$, $0 \le C_{\rm RL} \le 2.3$, $-1.5 \le C_{\rm T} \le 1.5$ and $-3.3 \le C_{\rm TE} \le 2.6$, and all of the remaining Wilson coefficients vary in the region $-\left|C_{10}^{\rm SM}\right| \le C_X \le \left|C_{10}^{\rm SM}\right|$.

It follows from the expressions of all forward–backward asymmetries of the leptons that explicit forms of the form factors are needed, which are the main and most important parameters in the calculation of $\mathcal{A}_{ij}$. These form factors are calculated in the framework of the QCD sum rules in [3,13,14] whose $q^2$ dependences are given as

$$g_(q^2) = \frac{1\,\text{GeV}}{\left(1 - \frac{q^2}{(5.6\,\text{GeV})^2}\right)^2},$$
$$f_(q^2) = \frac{0.8\,\text{GeV}}{\left(1 - \frac{q^2}{(6.5\,\text{GeV})^2}\right)^2},$$
$$g_1(q^2) = \frac{3.74\,\text{GeV}^2}{\left(1 - \frac{q^2}{40.5\,\text{GeV}^2}\right)^2},$$
$$f_1(q^2) = \frac{0.67\,\text{GeV}^2}{\left(1 - \frac{q^2}{30\,\text{GeV}^2}\right)^2},$$

which we will use in the numerical analysis.

Numerical results are presented only for the $B_s \to \ell^+\ell^-\gamma$ decay, because in the SU(3) limit the difference between the decay rates of $B_s \to \ell^+\ell^-\gamma$ and $B_d \to \ell^+\ell^-\gamma$ is attributed only to the CKM matrix elements. In other words, the decay rate of the $B_s \to \ell^+\ell^-\gamma$ is approximately 20 times larger compared to that of decay rate of $B_d \to \ell^+\ell^-\gamma$; that is

$$\frac{\Gamma(B_d\to\ell^+\ell^-\gamma)}{\Gamma(B_s\to\ell^+\ell^-\gamma)} \simeq \frac{|V_{tb}V_{td}^*|^2}{|V_{tb}V_{ts}^*|^2} \simeq \frac{1}{20}.$$

Concerning this ratio, we would like to make the following remark. If the contribution of the weak annihilation diagram (see for example [9]), as well as the CKM

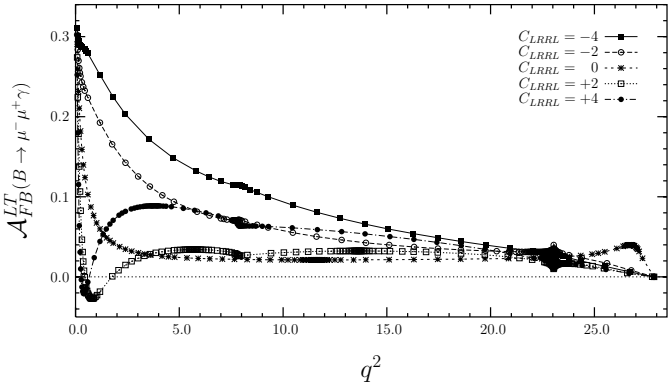


**Fig. 1.** The dependence of the polarized forward–backward asymmetry $\mathcal{A}_{\rm FB}^{\rm LT}$ on $q^2$ at four fixed values of $C_{\rm LRRL}$ for the $B_s \to \mu^+\mu^-\gamma$ decay

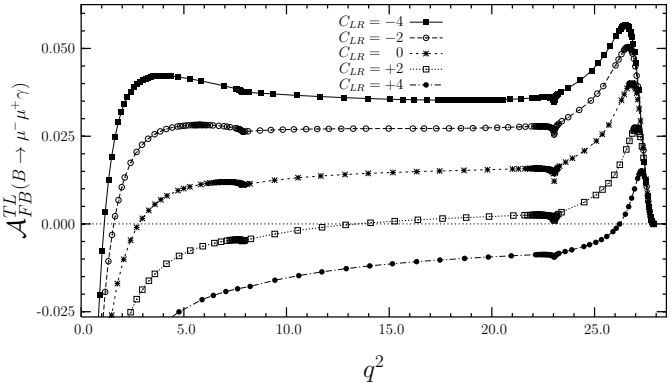


**Fig. 2.** The dependence of the polarized forward–backward asymmetry $\mathcal{A}_{\rm FB}^{\rm TL}$ on $q^2$ at four fixed values of $C_{\rm LR}$ for the $B_s \to \mu^+\mu^-\gamma$ decay

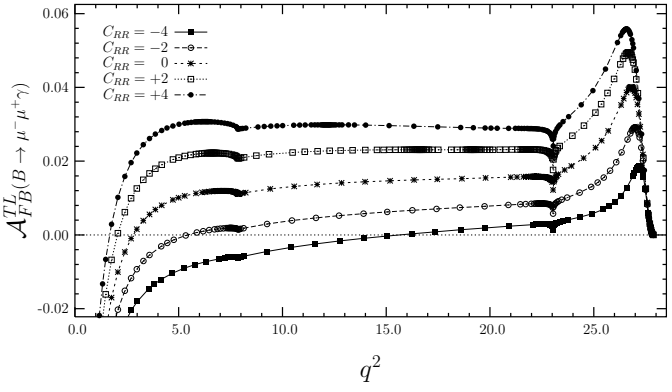


**Fig. 3.** The same as in Fig. 2, but for the coefficient $C_{\rm RR}$

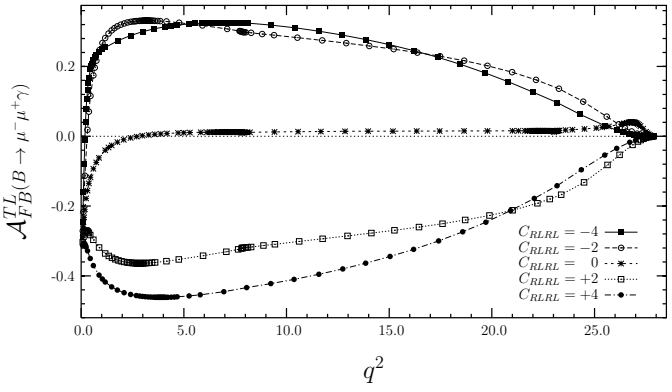


**Fig. 4.** The same as in Fig. 2, but for the coefficient $C_{\rm RLRL}$

factor in $Y^{\rm per}(\hat{s})$, is taken into account, $B_d \to \ell^+\ell^-\gamma$ and $B_s \to \ell^+\ell^-\gamma$ decay rates involve then different CKM factors. And if these contributions are neglected, which in fact are small, the above-mentioned ratio holds to within a good accuracy for the $B_q \to \ell^+\ell^-\gamma$ decay widths.

We now proceed by commenting on the result of our numerical analysis. Firstly, we study the dependence of the polarized forward–backward asymmetries on $q^2$ at five different values of the new Wilson coefficients. Our detailed numerical analysis shows that for the $B_s \to \mu^+\mu^-\gamma$ decay only the $\mathcal{A}_{\rm FB}^{\rm LT}$ and $\mathcal{A}_{\rm FB}^{\rm TL}$ asymmetries have zero positions (the numerical values of the asymmetries $\mathcal{A}_{\rm FB}^{\rm LN}$ and $\mathcal{A}_{\rm FB}^{\rm NL}$ are very small and hence we do not present them). In Fig. 1 we present the dependence of $\mathcal{A}_{\rm FB}^{\rm LT}$ on $q^2$ at five fixed values of the scalar interaction coefficient $C_{\rm LRRL} = -4; -2; 0; +2; +4$. From this figure we see that the zero position which occurs for positive values of $C_{\rm LRLR}$ is shifted to the left for increasing values of $C_{\rm LRLR}$. The same figure also depicts that the zero position of $\mathcal{A}_{\rm FB}^{\rm LT}$ is absent for the SM case. Therefore, determination of the zero position of $\mathcal{A}_{\rm FB}^{\rm LT}$ is an unambiguous indication of the new physics beyond the SM, as well as allowing us to determine the sign of the scalar interaction coefficients $C_{\rm LRRL}$. The numerical calculations show that, similar to the previous case, the zero position of the $\mathcal{A}_{\rm FB}^{\rm LT}$ appears again, but the difference from it being it occurs for the negative values of $C_{\rm RLRL}$. A more interesting observation for these cases is that the zero position appears for $q^2 < 2\,{\rm GeV}^2$ and hence it is free of the long distance $J/\psi$ contributions. It should be noted here that the zero position of $\mathcal{A}_{\rm FB}^{\rm LT}$ is present for the remaining scalar interaction coefficients $C_{\rm LRLR}$ and $C_{\rm RLLR}$ as well, but zero position of $\mathcal{A}_{\rm FB}^{\rm LT}$ appears at $q^2 \simeq 10\,{\rm GeV}^2$. As far as $B_s \to \mu^+\mu^-\gamma$ decay is concerned, our numerical analysis shows that the zero position of $\mathcal{A}_{\rm FB}^{\rm LT}$ is absent for all Wilson coefficients other than the scalar interaction coefficients. Hence, a determination of the zero position of $\mathcal{A}_{\rm FB}^{\rm LT}$ can serve as a good test for establishing new physics beyond the SM due to the presence of the scalar interaction coefficients.

The situation for the $\mathcal{A}_{\rm FB}^{\rm TL}$ asymmetry for the $B_s \to \mu^+\mu^-\gamma$ decay is richer in content compared to that of the $\mathcal{A}_{\rm FB}^{\rm LT}$ case. For this forward–backward asymmetry, the zero position occurs for all new Wilson coefficients. In Figs. 2–5 we present the dependence of $\mathcal{A}_{\rm FB}^{\rm TL}$ on $q^2$ at five fixed values of the new Wilson coefficients and we get the following results.

(1) For vector interactions with the Wilson coefficients $C_{\rm LL}$ and $C_{\rm RR}$, the zero position of $\mathcal{A}_{\rm FB}^{\rm TL}$ is shifted. When these coefficients get positive (negative) values, the zero position of $\mathcal{A}_{\rm FB}^{TL}$ is shifted to the left (right) compared to that of the SM case. In the presence of the Wilson coefficients $C_{\rm LR}$ and $C_{\rm RL}$ the zero position of the $\mathcal{A}_{\rm FB}^{\rm TL}$ is shifted to the right (left) compared to that of the SM result, when these Wilson coefficients are positive (negative).

(2) In the presence of the scalar interactions with the coefficients $C_{\rm LRRL}$ and $C_{\rm RLRL}$, the zero position of $\mathcal{A}_{\rm FB}^{\rm TL}$ is

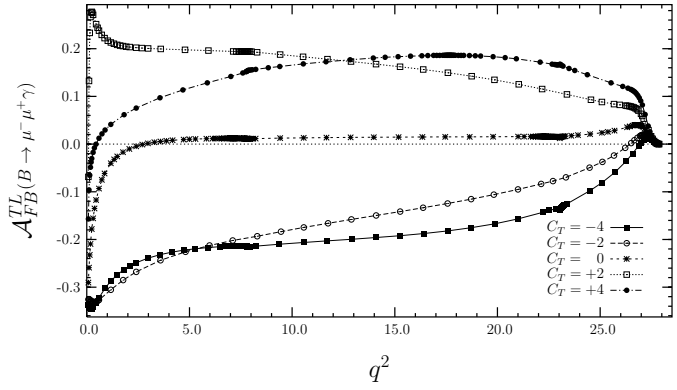


**Fig. 5.** The same as in Fig. 2, but for the coefficient $C_{\rm T}$

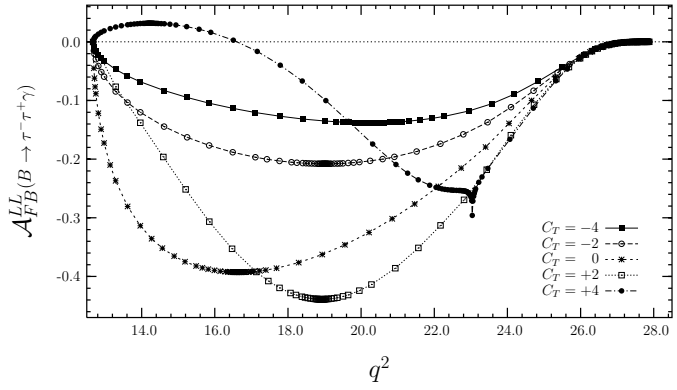


**Fig. 6.** The dependence of the polarized forward–backward asymmetry $\mathcal{A}_{\rm FB}^{\rm LL}$ on $q^2$ at four fixed values of $C_{\rm T}$ for the $B_s \to \tau^+\tau^-\gamma$ decay

shifted to the left compared to that of the SM result. The zero position for $C_{\rm LRRL}$ occurs only for its positive values, while it occurs only for the negative values of $C_{\rm RLRL}$.

In the presence of scalar interactions $C_{\rm RLLR}$ and $C_{\rm LRLR}$, no new zero position of $\mathcal{A}_{\rm FB}^{\rm TL}$ occurs with respect to the one for the SM case.

(3) New zero positions of $\mathcal{A}_{\rm FB}^{\rm TL}$ are observed in the presence of the tensor interaction for the positive values of $C_{\rm T}$, and the zero position is shifted to the left,

In the case of $B_s \to \tau^+\tau^-\gamma$ decay, similar to the $B_s \to \mu^+\mu^-\gamma$ decay, we observe that several of the polarized forward–backward asymmetries are very sensitive to the existence of new physics. Let us briefly summarize our results.

(i) $\mathcal{A}_{\rm FB}^{\rm LL}$ is sensitive to the presence of the tensor interaction and its zero position occurs for $C_{\rm T} = +4$ at $q^2 \approx 17\,{\rm GeV}^2$, while the zero position of $\mathcal{A}_{\rm FB}^{\rm LL}$ is absent for the SM case. Therefore, a determination of the zero position of $\mathcal{A}_{\rm FB}^{\rm LL}$ can confirm the existence of the tensor interaction in the $B_s \to \tau^+\tau^-\gamma$ decay (see Fig. 6).

(ii) Among all polarization asymmetries (which can be measurable in the experiments) only $\mathcal{A}_{\rm FB}^{\rm TL}$ is very sensitive to the existence of all types of new physics interactions, except to the presence of the vector interactions with coefficients $C_{\rm LL}$ and $C_{\rm RR}$.

(1) $\mathcal{A}_{\rm FB}^{\rm TL}$ exhibits similar dependence on $C_{\rm LR}$ and $C_{\rm RL}$. The zero position of $\mathcal{A}_{\rm FB}^{\rm TL}$ is shifted to the left (right) when $C_{\rm LR}$

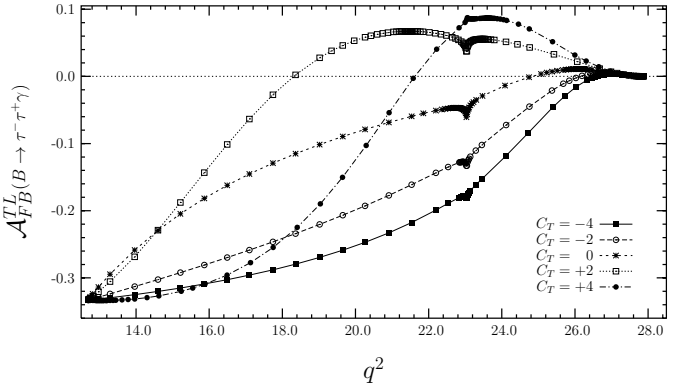


**Fig. 7.** The dependence of the polarized forward–backward asymmetry $\mathcal{A}_{\rm FB}^{\rm TL}$ on $q^2$ at four fixed values of $C_{\rm T}$ for the $B_s \to \tau^+\tau^-\gamma$ decay

and $C_{\rm RL}$ are negative (positive) compared to that of the SM prediction. Note that the zero position of $\mathcal{A}_{\rm FB}^{\rm TL}$ lies on the left side for the vector interaction $C_{\rm LR}$ compared to the zero position of the $C_{\rm RL}$.

(2) $\mathcal{A}_{\rm FB}^{\rm TL}$ shows a stronger dependence on the scalar interactions $C_{\rm LRRL}$ and $C_{\rm RLRL}$. The magnitude of $\mathcal{A}_{\rm FB}^{\rm TL}$ increases (decreases) as the new Wilson coefficient $C_{\rm LRRL}$ gets positive (negative) values. This behavior is to the contrary for the coefficient $C_{\rm RLRL}$.

(3) In the presence of the tensor interaction with the coefficient $C_{\rm T}$, zero position of the asymmetry $\mathcal{A}_{\rm FB}^{\rm TL}$ is located on the left side of the SM prediction for negative values of $C_{\rm T}$ (Fig. 7).

We see from the explicit expressions of the polarized forward–backward asymmetries that they all depend both on $q^2$ and the new Wilson coefficients. For this reason there may appear difficulties in the experiments in studying the dependence of the physical observables on both parameters simultaneously. In order to get "pure information" about new physics, we eliminate the dependence of physical quantities on $q^2$, by performing the integration over $q^2$ in the kinematically allowed region, i.e., we average the polarized forward–backward asymmetry

$$\langle \mathcal{A}_{ij} \rangle = \frac{\int_{4m_\ell^2}^{m_B^2} \mathcal{A}_{ij} \dfrac{{\rm d}\mathcal{B}}{{\rm d}q^2} {\rm d}q^2}{\int_{4m_\ell^2}^{m_B^2} \dfrac{{\rm d}\mathcal{B}}{{\rm d}q^2} {\rm d}q^2}.$$

In Fig. 8 we depict the dependence of $\langle \mathcal{A}_{\rm FB}^{\rm LL} \rangle$ on the new Wilson for the $B_s \to \mu^+\mu^-\gamma$ decay. From this figure we see that $\langle \mathcal{A}_{\rm FB}^{\rm LL} \rangle$ shows a symmetric behavior in its dependence on all scalar interactions; and except for the regions $-4 < C_{\rm RR}, C_{\rm RL} < 0$, $-0.4 < C_{\rm LRRL}, C_{\rm LRRL} < 0$ and $0 \le C_{\rm RLRL}, C_{\rm LRLR} < 0.4$ it is larger compared to the SM result (the SM result corresponds to the intersection point of all curves). It is also interesting to observe that $\langle \mathcal{A}_{\rm FB}^{\rm LL} \rangle > \langle \mathcal{A}_{\rm FB}^{\rm SM} \rangle$ for only negative values of $C_{\rm RR}$.

Our numerical analysis furthermore shows that, for the $B_s \to \mu^+\mu^-\gamma$ decay, $\langle \mathcal{A}_{\rm FB}^{\rm LT} \rangle$ is sensitive only to $C_{\rm T}$ and at negative (positive) values of $C_{\rm T}$ $\langle \mathcal{A}_{\rm FB}^{\rm LT} \rangle$ is positive (negative) and larger (smaller) compared to the SM result.

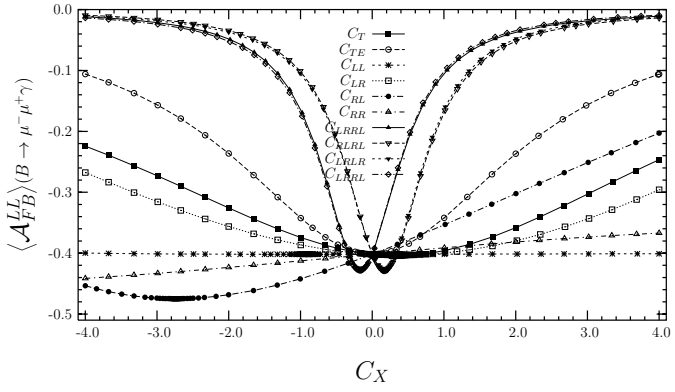


**Fig. 8.** The dependence of the polarized forward–backward asymmetry $\mathcal{A}_{\rm FB}^{\rm LL}$ on the new Wilson coefficients for the $B_s \to \mu^+\mu^-\gamma$ decay

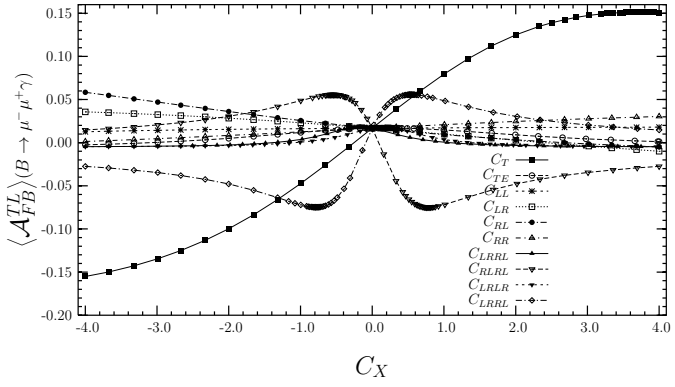


**Fig. 9.** The same as in Fig. 8, but for the polarized forward–backward asymmetry $\mathcal{A}_{\rm FB}^{\rm TL}$

Therefore, determination of the sign and magnitude of $\langle \mathcal{A}_{\rm FB}^{\rm LT} \rangle$ can serve as a good test for establishing existence of the tensor interaction.

The dependence of $\langle \mathcal{A}_{\rm FB}^{\rm TL} \rangle$ on the new Wilson coefficients for the $B_s \to \mu^+\mu^-\gamma$ decay is presented in Fig. 9. We observe from this figure that $\langle \mathcal{A}_{\rm FB}^{\rm TL} \rangle$ shows stronger dependence on the tensor interaction coefficient $C_{\rm T}$ and scalar interactions $C_{\rm RLRL}$ and $C_{\rm LRRL}$.

In Figs. 10, 11, and 12 we present the dependence of $\langle \mathcal{A}_{\rm FB}^{\rm LL} \rangle$, $\langle \mathcal{A}_{\rm FB}^{\rm LT} \rangle$ and $\langle \mathcal{A}_{\rm FB}^{\rm TL} \rangle$ on the new Wilson coefficients for the $B_s \to \tau^+\tau^-\gamma$ decay, respectively. Figure 10 depicts that $\langle \mathcal{A}_{\rm FB}^{\rm LL} \rangle$ exhibits considerable departure from the SM result for the scalar interactions and the vector interaction with coefficient $C_{\rm RR}$. We see from Fig. 11 that when new Wilson coefficients are negative $\langle \mathcal{A}_{\rm FB}^{\rm LT} \rangle$ shows a stronger dependence on the tensor interaction ($C_{\rm T}$) and scalar type interactions, and when $C_X > 0$, $\langle \mathcal{A}_{\rm FB}^{\rm LT} \rangle$ exhibits a strong dependence on vector interactions and the tensor interaction with the coefficient $C_{\rm TE}$.

At the end of this section, we discuss the problem of the detectability of forward–backward asymmetry in the experiments. Experimentally, to measure an asymmetry $\langle \mathcal{A}_{ij} \rangle$ of the decay with the branching ratio $\mathcal{B}$ at $n\sigma$ level, the required number of events (i.e., the number of $B\bar{B}$ pairs) is given by

$$\mathcal{N} = \frac{n^2}{\mathcal{B} s_1 s_2 \langle \mathcal{A}_{ij} \rangle^2},$$

where $s_1$ and $s_2$ are the efficiencies of the leptons. The efficiency of the $\mu$-lepton is practically equal to one, and typical values of the efficiency of the $\tau$-lepton ranges from 50% to 90% for the various decay modes [21].

From the expression for $\mathcal{N}$ we see that, in order to obtain the forward–backward asymmetries in $B_s \to \ell^+\ell^-\gamma$ decays at $3\sigma$ level, the minimum number of required events are (for the efficiency of $\tau$-lepton we take 0.5, and for $\langle \mathcal{A}_{ij} \rangle$, their maximal values beyond the SM)

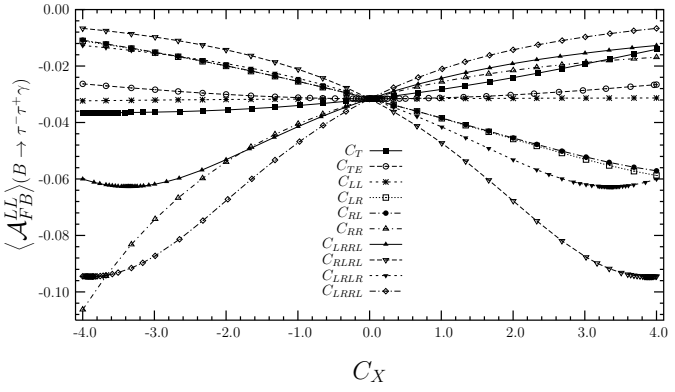


**Fig. 10.** The same as in Fig. 8, but for the $B_s \to \tau^+\tau^-\gamma$ decay

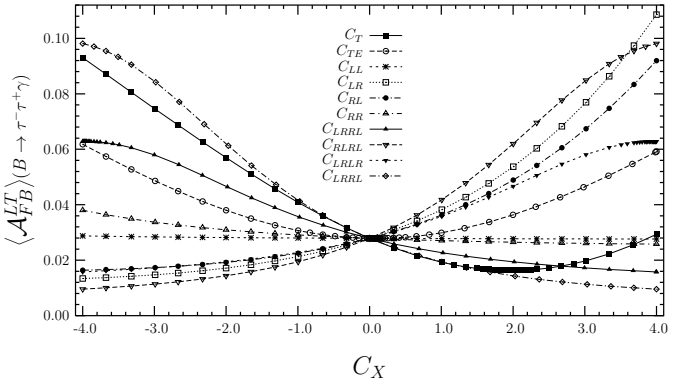


**Fig. 11.** The same as in Fig. 10, but for the polarized forward–backward asymmetry $\mathcal{A}_{\rm FB}^{\rm LT}$

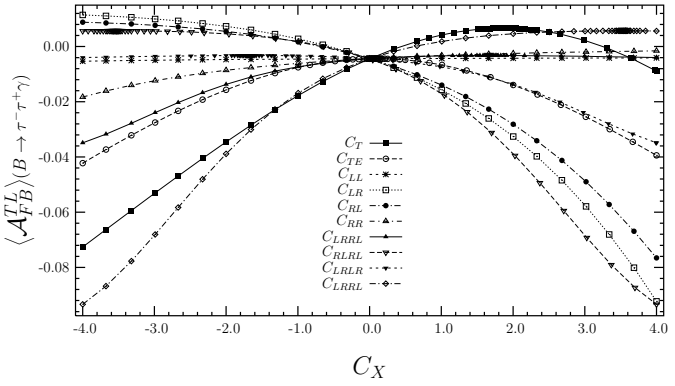


**Fig. 12.** The same as in Fig. 10, but for the polarized forward–backward asymmetry $\mathcal{A}_{\rm FB}^{\rm TL}$

(1) for the $B_s \to \mu^+\mu^-\gamma$ decay

$$\mathcal{N} = \begin{cases} \sim 2 \times 10^9 \ \ \langle \mathcal{A}_{\rm LL} \rangle \,, \\ \sim 3 \times 10^{10} \, \langle \mathcal{A}_{\rm LT} \rangle \simeq \langle \mathcal{A}_{\rm TL} \rangle \,, \end{cases}$$

which yields that, for detecting $\langle \mathcal{A}_{\rm LT} \rangle$ and $\langle \mathcal{A}_{\rm TL} \rangle$, more than $10^{13}$ $\bar{B}B$ pairs are required. Next,
(2) for $B_s \to \tau^+\tau^-\gamma$ decay

$$\mathcal{N} = \sim 6 \times 10^{11} \, \langle \mathcal{A}_{\rm LL} \rangle \,, \ \ \langle \mathcal{A}_{\rm LT} \rangle \,, \ \ \langle \mathcal{A}_{\rm TL} \rangle \,.$$

The number of $\bar{B}B$ pairs that will be produced at LHC is around $\sim 10^{12}$. As a result of a comparison of this number of $\bar{B}B$ pairs with that of $\mathcal{N}$, we conclude that $\langle \mathcal{A}_{\rm LL} \rangle$, $\langle \mathcal{A}_{\rm TL} \rangle$ and $\langle \mathcal{A}_{\rm TL} \rangle$ in both decays can be detectable in "beyond the SM scenarios" in future experiments at LHC. Note that in the SM, only $\langle \mathcal{A}_{\rm LL} \rangle$ for the $B_s \to \mu^+\mu^-\gamma$ decay can be detectable at LHC. Therefore, the observation of these asymmetries can be explained only by new physics beyond the SM.

In conclusion, we calculate polarized forward–backward asymmetries using the most general, model independent form of the effective Hamiltonian including all possible form of interactions. The sensitivity of the averaged polarized forward–backward asymmetries to the new Wilson coefficients is studied. Finally we discuss the possibility of experimental measurement of these double-lepton polarization asymmetries at LHC.

## References


1. M. Battaglia et al., hep-ph/0304132 (2003)
2. P. Ball et al., B Decays, in: Proceedings of the workshop on Standard Model Physics (and more) at the LHC, CERN 2000–004 (2000)
3. T.M. Aliev, A. Özpineci, M. Savcı, Phys. Rev. D **55**, 7059 (1997)
4. C.Q. Geng, C.C. Lih, Wei-Min Zhang, Phys. Rev. D **62**, 074017 (2000)
5. Y. Dincer, L.M. Sehgal, Phys. Lett. B **521**, 7 (2000)
6. S. Descotes-Genon, C.T. Sachrajda, Phys. Lett. B **557**, 213 (2003)
7. F. Krüger, D. Melikhov, Phys. Rev. D **67**, 034002 (2003)
8. T.M. Aliev, A. Özpineci, M. Savcı, Phys. Lett. B **520**, 69 (2001); Eur. J. Phys. C **27**, 405 (2003); G. Eilam, C.D. Lu, D.X. Zhang, Phys. Lett. B **391**, 461 (1997)
9. D. Melikhov, N. Nikitin, Phys. Rev. D **70**, 114028 (2004)
10. W. Bensalem, D. London, N. Sinha, R. Sinha, Phys. Rev. D **67**, 034007 (2003)
11. T.M. Aliev, V. Bashiry, M. Savcı, hep-ph/0411327 (2004)
12. S. Fukae, C.S. Kim, T. Morozumi, T. Yoshikawa, Phys. Rev. D **59**, 074013 (1999)
13. G. Eilam, I. Halperin, R.R. Mendel, Phys. Lett. B **361**, 137 (1995)
14. T.M. Aliev, N.K. Pak, M. Savcı, Phys. Lett. B **424**, 175 (1998)
15. C.S. Lim, T. Morozumi, A.I. Sanda, Phys. Lett. B **218**, 343 (1989); N.G. Deshpande, J. Trampetic, K. Panose, Phys. Rev. D **39**, 1461 (1989); A.I. Vainshtein, V.I. Zakharov, L.B. Okun, M.A. Shifman, Sov. J. Nucl. Phys. **24**, 427 (1976)
16. A.J. Buras, M. Münz, Phys. Rev. D **52**, 186 (1995)
17. A. Ali, P. Ball, L.T. Handoko, G. Hiller, Phys. Rev. D **61**, 074024 (2000)
18. A. Ishikawa et al., BELLE Collaboration, Phys. Rev. Lett. **91**, 261601 (2003)
19. B. Aubert et al., BaBar Collaboration, Phys. Rev. Lett. **91**, 221802 (2003)
20. M.C. Chang et al., BELLE Collaboration, Phys. Rev. D **67**, 111101 (2003)
21. G. Abbiendi et al., OPAL Collaboration, Phys. Lett. B **492**, 23 (2000)